


**First Direct Measurement of the 64.5 keV Resonance Strength in the  $^{17}\text{O}(p,\gamma)^{18}\text{F}$  Reaction**

R. M. Gesuè<sup>1,2</sup>, G. F. Ciani,<sup>3,4,\*</sup> D. Piatti<sup>5,6,†</sup>, A. Boeltzig,<sup>7</sup> D. Rapagnani,<sup>8,9</sup> M. Aliotta,<sup>10</sup> C. Ananna,<sup>8,9</sup> L. Barbieri,<sup>10</sup> F. Barile,<sup>4</sup> D. Bemmerer,<sup>7</sup> A. Best,<sup>8,9</sup> C. Brogini,<sup>6</sup> C. G. Bruno,<sup>10</sup> A. Cacioli,<sup>5,6</sup> M. Camprostrini,<sup>11</sup> F. Casaburo,<sup>12,13</sup> F. Cavanna,<sup>14</sup> P. Colombetti,<sup>15,14</sup> A. Compagnucci,<sup>1,2</sup> P. Corvisiero,<sup>12,13</sup> L. Csedreki,<sup>16</sup> T. Davinson,<sup>10</sup> G. M. De Gregorio,<sup>17,18</sup> D. Dell'Aquila,<sup>8,9</sup> R. Depalo,<sup>17,18</sup> A. Di Leva,<sup>8,9</sup> Z. Elekes,<sup>16,19</sup> F. Ferraro,<sup>2</sup> A. Formicola,<sup>20</sup> Zs. Fülöp,<sup>16</sup> G. Gervino,<sup>15,14</sup> A. Guglielmetti,<sup>17,18</sup> C. Gustavino,<sup>20</sup> Gy. Gyürky,<sup>16</sup> G. Imbriani,<sup>8,9</sup> M. Junker,<sup>2</sup> M. Lugaro,<sup>21,22</sup> P. Marigo,<sup>5,6</sup> J. Marsh,<sup>10</sup> E. Masha,<sup>7</sup> R. Menegazzo,<sup>6</sup> D. Mercogliano,<sup>8,9</sup> V. Paticchio,<sup>4</sup> R. Perrino,<sup>4,‡</sup> P. Prati,<sup>12,13</sup> V. Rigato,<sup>11</sup> D. Robb,<sup>10</sup> L. Schiavulli,<sup>3,4</sup> R. S. Sidhu,<sup>10</sup> J. Skowronski,<sup>5,6</sup> O. Straniero,<sup>23,20</sup> T. Szücs,<sup>16</sup> and S. Zavatarelli<sup>13,12</sup>

(LUNA Collaboration)

<sup>1</sup>Gran Sasso Science Institute, 67100 L'Aquila, Italy<sup>2</sup>INFN, Laboratori Nazionali del Gran Sasso, 67100 Assergi, Italy<sup>3</sup>Università degli Studi di Bari "A. Moro," 70125 Bari, Italy<sup>4</sup>INFN, Sezione di Bari, 70125 Bari, Italy<sup>5</sup>Università degli Studi di Padova, 35131 Padova, Italy<sup>6</sup>INFN, Sezione di Padova, 35131 Padova, Italy<sup>7</sup>Helmholtz-Zentrum Dresden-Rossendorf, 01328 Dresden, Germany<sup>8</sup>Università degli Studi di Napoli "Federico II," 80125 Naples, Italy<sup>9</sup>INFN, Sezione di Napoli, 80125 Naples, Italy<sup>10</sup>SUPA, School of Physics and Astronomy, University of Edinburgh, EH9 3FD Edinburgh, United Kingdom<sup>11</sup>Laboratori Nazionali di Legnaro, 35020 Legnaro, Italy<sup>12</sup>Università degli Studi di Genova, 16146 Genova, Italy<sup>13</sup>INFN, Sezione di Genova, 16146 Genova, Italy<sup>14</sup>INFN, Sezione di Torino, 10125 Torino, Italy<sup>15</sup>Università degli Studi di Torino, 10125 Torino, Italy<sup>16</sup>HUN-REN Institute for Nuclear Research (HUN-REN ATOMKI), PO Box 51, H-4001 Debrecen, Hungary<sup>17</sup>Università degli Studi di Milano, 20133 Milano, Italy<sup>18</sup>INFN, Sezione di Milano, 20133 Milano, Italy<sup>19</sup>Institute of Physics, Faculty of Science and Technology, University of Debrecen, Egyetem tér 1., H-4032 Debrecen, Hungary<sup>20</sup>INFN, Sezione di Roma, 00185 Roma, Italy<sup>21</sup>Konkoly Observatory, Research Centre for Astronomy and Earth Sciences (CSFK), HUN-REN, and MTA Centre for Excellence, 1121 Budapest, Hungary<sup>22</sup>ELTE Eötvös Loránd University, Institute of Physics, 1117 Budapest, Hungary<sup>23</sup>INAF-Osservatorio Astronomico d'Abruzzo, 64100 Teramo, Italy (Received 6 March 2024; revised 14 May 2024; accepted 18 June 2024; published 30 July 2024)

The CNO cycle is one of the most important nuclear energy sources in stars. At temperatures of hydrostatic H-burning ( $20 \text{ MK} < T < 80 \text{ MK}$ ) the  $^{17}\text{O}(p,\gamma)^{18}\text{F}$  reaction rate is dominated by the poorly constrained 64.5 keV resonance. Here, we report on the first direct measurements of its resonance strength and of the direct capture contribution at 142 keV, performed with a new high sensitivity setup at LUNA. The present resonance strength of  $\omega\gamma_{(p,\gamma)}^{\text{bare}} = (30 \pm 6_{\text{stat}} \pm 2_{\text{syst}}) \text{ peV}$  is about a factor of 2 higher than the values in literature, leading to a  $\Gamma_p^{\text{bare}} = (34 \pm 7_{\text{stat}} \pm 3_{\text{syst}}) \text{ neV}$ , in agreement with the LUNA result from the  $(p,\alpha)$  channel. Such agreement strengthens our understanding of the oxygen isotopic ratios measured in red giant stars and in O-rich presolar grains.

DOI: [10.1103/PhysRevLett.133.052701](https://doi.org/10.1103/PhysRevLett.133.052701)\*Contact author: [giovanni.ciani@ba.infn.it](mailto:giovanni.ciani@ba.infn.it)†Contact author: [denise.piatti@pd.infn.it](mailto:denise.piatti@pd.infn.it)

‡Permanent address: INFN Sezione di Lecce, 73100 Lecce, Italy.

The CNO cycle releases the energy necessary to sustain the luminosity of red giant, the asymptotic giant branch, and supergiant stars, and of main-sequence stars with mass  $M > 1.2M_{\odot}$ . It also powers extended convective zones, such as the convective core of the aforementioned main

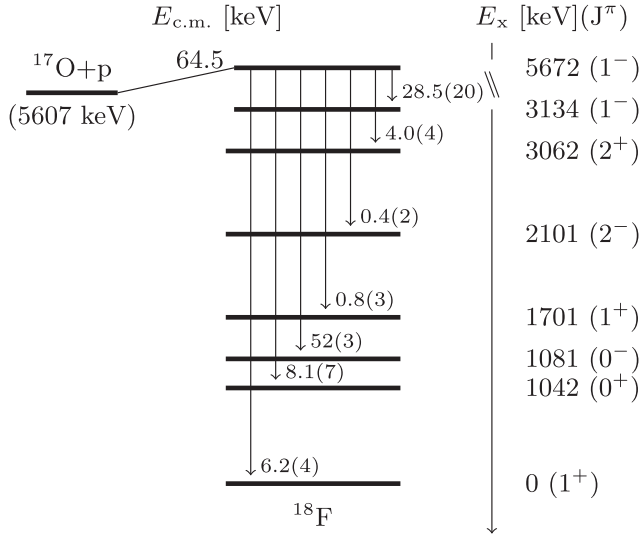


FIG. 1. Level scheme of  $^{18}\text{F}$  with primary branching ratios as reported in [12].

sequence stars and the convective envelopes of red giants and supergiants. Molecular lines observed in the infrared allows for the measurements of the isotopic composition of selected elements in stars [1]. The measurements of C, N, and O isotopic ratios, in particular, provide a unique tool to understand the interplay between internal nuclear burning and various physical processes producing deep mixing in giant stars. A successful application of this probe in stellar astrophysics requires precise measurements of the burning rates of all the reactions of the CNO cycle.

In this Letter, we present the first direct measurement of the strength of the narrow resonance at  $E_r = 64.5$  keV [2] in the  $^{17}\text{O}(p, \gamma)^{18}\text{F}$  reaction ( $Q$  value = 5607.1(5) keV [3]), corresponding to the  $E_x = 5671.6(2)$  keV [4] level in  $^{18}\text{F}$  (Fig. 1). At the temperatures of the stellar hydrostatic H-burning,  $T \cong 20\text{--}80$  MK [5], this nuclear state dominates the rates of the two  $^{17}\text{O}$  destruction channels in the CNO cycle:  $^{17}\text{O}(p, \gamma)^{18}\text{F}$  and  $^{17}\text{O}(p, \alpha)^{14}\text{N}$ . These rates contribute to determine the  $^{16}\text{O}/^{17}\text{O}$  isotopic ratio observed in giant stars [6–8] and in stardust grains that form in the material lost by these stars and are recovered from meteorites [9]. Attributing the stardust grain origin to a specific scenario is, in fact, particularly sensitive to the choice for the  $^{17}\text{O} + p$  reaction rates [10]. Reducing their uncertainty would allow us to disentangle the origin of oxide stardust grains from evolved stars of mass lower than  $\sim 1.5M_\odot$ , thereby proving the existence of extra mixing below the border of the convective envelope, and/or from evolved stars of mass above  $\sim 4M_\odot$ , where the CNO cycle occurs at the base of the convective envelope itself [10,11].

Previously, the  $^{17}\text{O}(p, \gamma)^{18}\text{F}$  reaction was investigated down to  $E = 150$  keV through prompt  $\gamma$ -ray detection or through off-line counting of  $^{18}\text{F}$  decays from irradiated targets (activation method) [4,13–18]. Despite

experimental efforts, the resonance strength at  $E_r = 64.5$  keV in the  $(p, \gamma)$  channel ( $\omega\gamma_{(p,\gamma)}$ ) has never been directly measured. The presently adopted value was determined through the following relation, after having observed that for the partial widths  $\Gamma_\alpha \gg \Gamma_p, \Gamma_\gamma$  [13,18–21]:

$$\omega\gamma_{(p,\gamma)} = \frac{(2J_x + 1)}{(2J_p + 1)(2J_{^{17}\text{O}} + 1)} \frac{\Gamma_p \Gamma_\gamma}{\Gamma_\alpha}. \quad (1)$$

The energy  $E_x = 5671.6(2)$  keV and spin  $J_x = 1^-$  of the  $^{18}\text{F}$  excited state for the resonance of interest were obtained by studying the  $^{14}\text{N}(\alpha, \gamma)^{18}\text{F}$ ,  $^{17}\text{O}(p, \gamma)^{18}\text{F}$ , and  $^{17}\text{O}(^3\text{He}, p\gamma)^{18}\text{F}$  reactions [13,22,23]. The  $\Gamma_\alpha = 130(5)$  eV and  $\Gamma_\gamma = 0.44(2)$  eV widths were measured via the  $^{14}\text{N} + \alpha$  channels [22,24].

The most uncertain quantity in Eq. (1) is the proton width  $\Gamma_p$ , which is estimated from the strength of the  $E_r = 64.5$  keV resonance in the  $(p, \alpha)$  channel, since  $\omega\gamma_{(p,\alpha)} \propto \Gamma_p$ . A discrepancy of a factor 2 and 2.5 exists between the recent result by LUNA [25] and values reported by previous direct [18,19] and indirect measurements [20], respectively, see Table I. A new independent direct measurement of the 64.5 keV resonance strength in the  $^{17}\text{O}(p, \gamma)^{18}\text{F}$  channel is needed to address this tension. However, due to the low expected count rate, such a direct measurement requires an optimized setup providing both an ultralow background and an extremely high detection efficiency.

In the following, we present the first direct measurement of the 64.5 keV resonance strength performed at the Laboratory for Underground Nuclear Astrophysics (LUNA), located at the Laboratori Nazionali del Gran Sasso (LNGS, Italy).

The LUNA deep-underground location guarantees a muon (and neutron) background level 6 (and 3) orders of magnitude lower than above ground [31,32]. A detailed description of the setup and the achieved sensitivity can be found in [33]; here we only report its main features.

A high-intensity proton beam (average current on target  $I = 200$   $\mu\text{A}$ ) was provided by the LUNA-400 kV accelerator [34]. The beam was analyzed, collimated, and then sent through a copper pipe, extending to a distance of 1 cm from the target. The pipe was biased to  $-300$  V and kept at liquid nitrogen temperature to work both as secondary electron suppression and as a cold trap. The beam impinged on a water cooled solid target. The target holder and the scattering chamber were made of aluminum to minimize the  $\gamma$ -ray absorption providing an increase of efficiency with respect to previous setups of about a factor 4 [33,35]. Moreover, the scattering chamber and the target were electrically insulated from the beam line and functioned as a Faraday cup for beam current measurement.

The targets were produced at LNGS by anodic oxidation of tantalum backings, previously cleaned with an acid

TABLE I. Literature data for the  $E_r = 64.5$  keV resonance in the  $^{17}\text{O}(p,\gamma)^{18}\text{F}$  reaction: excitation energy  $E_x$ , spin-parity  $J^\pi$ , partial widths  $\Gamma_{\alpha,\gamma,p}$ , and resonance strength  $\omega\gamma_{(p,\gamma)}$ . For the proton width  $\Gamma_p$  and the resonance strength, when explicitly reported, the results corrected for the screening effect are also listed. For the present result the screening correction  $f = 1.15$  was estimated by applying the adiabatic approximation [26].

Reference	$E_x$ [keV]	$J^\pi$	$\Gamma_\alpha$ [eV]	$\Gamma_\gamma$ [eV]	$\Gamma_p$ [neV]	$\Gamma_p^{\text{bare}}$ [neV]	$\omega\gamma_{(p,\gamma)}$ [peV]	$\omega\gamma_{(p,\gamma)}^{\text{bare}}$ [peV]
[27]				0.45(5)				
[28]	5669(2)			0.47(10)				
[22]		$1^-$	200(60)	0.46(6)				
[24]			130(5)					
[29]				0.45(2)				
[23]	5672.57(32)							
[19]					22(4)			
[30]					21(2) <sup>a</sup>			
[4]	5671.6(2)							
[13,18,21]				0.44(2) <sup>b</sup>		19(3) <sup>c</sup>		16(3)
[20]						14(2) <sup>d</sup>		11.8(21)
[25]					40(7)	35(6)		
Present work					39(9)	34(8)	34(8)	30(6)

<sup>a</sup>Reanalysis of the experimental work by [19].

<sup>b</sup>Average value of the results in [22,27–29].

<sup>c</sup>Reanalysis of the experimental work by [19] taking into account the method described in [30] and correcting for the screening effect.

<sup>d</sup>Calculated by present authors starting from the reported  $\omega\gamma_{(p,\alpha)}$  and Eq. (1).

bath in isotopically  $^{17}\text{O}$  enriched water doped with 4% of  $^{18}\text{O}$  [36]. This procedure was proven to provide targets with a well known stoichiometry,  $\text{Ta}_2\text{O}_5$ , and a well defined thickness-voltage relation [36]. The well known  $E_r = 143$  keV resonance in the  $^{18}\text{O}(p,\gamma)^{19}\text{F}$  channel [37,38] was used to characterize the target thickness. Targets with two different thicknesses were used:  $\Delta E_{\text{lab}} = 21(1)$  and  $53(1)$  keV at 143 keV, corresponding to 147 and 378 nm, respectively [39]. To monitor the target degradation during the measurement a resonance scan of the aforementioned resonance was performed periodically, i.e., after every  $\approx 10$  C accumulated charge on target. The target degradation observed at  $E_r = 143$  keV can be directly related to the degradation at  $E_r = 64.5$  keV, since the stopping powers are known and the energy loss at the two energies is nearly the same (within 10% [39]). Targets were replaced after about 25 C of accumulated charge to guarantee the stability of the target stoichiometry within the layer where the 64.5 keV resonance was populated using an  $E_p = 80$  keV beam, see Fig. 2.

To characterize and monitor the target isotopic enrichment in  $^{17}\text{O}$ , dedicated runs were acquired periodically at  $E_p = 200$  keV, populating the  $E_r = 183$  keV resonance of  $^{17}\text{O}(p,\gamma)^{18}\text{F}$ . This resonance has a known strength of  $\omega\gamma_{(p,\gamma)} = (1.67 \pm 0.12) \mu\text{eV}$  [17]. The resulting experimental isotopic abundances of  $^{17}\text{O}$  in the three batches of targets are 87(1)%, 72(1)%, and 85(1)%, where only statistical uncertainties are reported.

To detect the  $\gamma$  rays from the  $^{17}\text{O}(p,\gamma)^{18}\text{F}$  reaction a high efficiency  $4\pi$  bismuth germanate oxide (BGO) summing detector was installed around the target and the scattering

chamber. The BGO is segmented into six optically independent crystals, each read out by a photomultiplier tube and a digital data acquisition chain [32,33,40,41]. The energy deposited and the time stamp of each event were recorded and used to produce a spectrum of coincident events in different crystals, hereafter referred to as the add-back spectrum [32]. The dead time, less than 1%, was determined using a pulser signal connected to the test input of each preamplifier and to a dedicated acquisition chain.

Finally, the whole setup was surrounded by a three-layer shielding to further reduce the  $\gamma$ -ray background, mainly due to reactions induced by environmental neutrons [32].

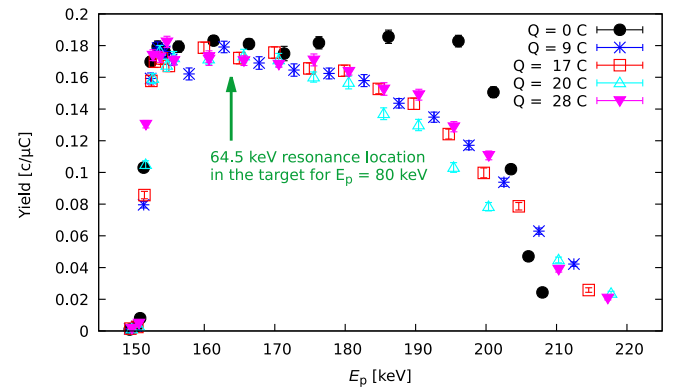


FIG. 2. Thick-target scans of the  $E_r = 143$  keV resonance in the  $^{18}\text{O}(p,\gamma)^{19}\text{F}$ . Scans were acquired after different amounts of charge deposited on target, and always before and after a long run on the  $E_r = 64.5$  keV resonance. Only the statistical uncertainty is plotted. The green arrow shows the beam energy at which the resonance was populated at  $E_p = 80$  keV.

The shield was composed, from inner to outer, of a 1 cm thick borated polyethylene (BPE) layer, a 10 cm thick lead shell and a 5 cm thick BPE cover [33].

A simulation of the setup was developed using the Geant4 framework [42]. The simulation was validated for  $\gamma$ -ray energies up to 7.6 MeV using  $^{137}\text{Cs}$  and  $^{60}\text{Co}$  calibrated source and the  $E_r = 259$  keV resonance of the  $^{14}\text{N}(p,\gamma)^{15}\text{O}$  reaction [43]. The simulation allowed us to characterize the BGO efficiency within 3% uncertainty [33].

The data taking covered four months, with an overall accumulated charge of 420 C on isotopically enriched  $^{17}\text{O}$  targets and 300 C ultrapure water (UPW) targets to investigate beam induced background, see below for details. Long runs ( $\sim 12$  h each) were performed at  $E_p = 80$  keV to populate the 64.5 keV resonance. Scans of the 143 keV resonance and runs on top of the 183 keV resonance were performed between the long runs to monitor the target degradation.

The 64.5 keV resonance strength is determined from the experimental yield  $Y_{\text{exp}}$  using the infinitely-thick-target approximation, i.e., the resonance width (130 eV) is much smaller than the target thickness (53 and 21 keV):

$$Y_{\text{exp}} = \frac{N_\gamma}{Q} = \frac{\lambda^2}{2e\epsilon_{\text{eff}}} \omega\gamma_{(p,\gamma)}\eta W, \quad (2)$$

where  $N_\gamma$  is the number of net counts,  $Q$  the accumulated charge,  $e$  the elementary charge, and  $\eta$  the detection efficiency. The angular distribution term  $W$  is 1 since the BGO covers most of the solid angle,  $\lambda$  represents the de Broglie wavelength at the center-of-mass resonant energy, and  $\epsilon_{\text{eff}}$  is the effective stopping power calculated using SRIM-v.13 database [39].

The yield from the 64.5 keV resonance was expected to be less than 0.3 counts/C [21]. Therefore, defining the region of interest (ROI) in the gamma energy spectra was critical. The long runs were precisely calibrated up to  $E_\gamma = 8$  MeV using the 143 keV resonance spectra, acquired before and after long runs allowing us to monitor possible gain shift. The regions of interest were determined via a dedicated study of BGO resolution and via simulation of the  $E_x = 5671.6(2)$  keV deexcitation cascades (Fig. 1).

To monitor possible beam induced background in the ROI, targets were produced by performing the anodic oxidation in a solution of UPW and water enriched in  $^{18}\text{O}$  at the 80% level. The UPW targets had the same thicknesses as  $^{17}\text{O}$  targets but a negligible amount of  $^{17}\text{O}$  isotope. A comparison of the summed add-back spectra acquired on  $^{17}\text{O}$  and UPW targets is shown in Fig. 3. A peak centered at the energy of interest,  $E_x = 5671.6(2)$  keV, is also visible in the UPW target spectra. This was attributed to a  $^2\text{H}$  contamination in the tantalum backings [44]. Because of the low BGO resolution, the  $^2\text{H}(p,\gamma)^3\text{He}$  reaction ( $Q$  value = 5493.475 08(6) keV [3]) peak cannot

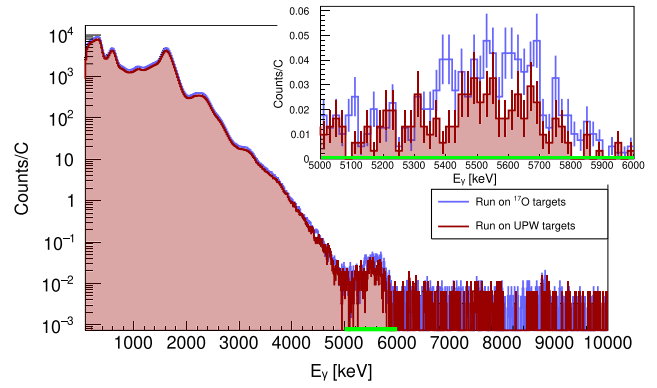


FIG. 3. Comparison between the add-back spectra acquired on  $^{17}\text{O}$  and UPW targets, in logarithmic scale. A peak is visible in the energy region of interest, highlighted in green and shown in the inset in linear scale.

be distinguished from the  $^{17}\text{O}(p,\gamma)^{18}\text{F}$  resonance peak at present beam energy. The deuterium contamination in tantalum was estimated to be of few parts per million, too low to be eliminated via mechanical or chemical methods. The identification of beam induced background takes advantage of both the segmentation of the BGO detector and the knowledge of the decay scheme of the resonant state of interest of  $^{18}\text{F}$  isotope [12]. This analysis is described in detail in [33], and used in [45–47]. In short, we implemented the method as follows: first the events with total energy in the sum peak ROI were selected; second, among these, we selected the events having deposited, in a single crystal, an energy corresponding to the 1081 and 1042 keV states ( $3300 \leq E_\gamma \leq 4850$  keV), see Fig. 4. We applied the method to the simulations to obtain the gate efficiency,  $24.3\% \pm 0.7\%$ . This approach allows for complete discrimination between events belonging to the  $^{17}\text{O}(p,\gamma)^{18}\text{F}$  reaction and those produced by the  $^2\text{H}(p,\gamma)^3\text{He}$  direct capture, since the latter proceeds solely to the ground state emitting one  $\gamma$  ray. A downside of the method is a loss of statistics, since the states we gated on have an overall intensity of 60.1(37)% [12]. The background that survived the second gate is due to random coincidences, mimicking the cascade of interest. We estimated and subtracted this contribution applying the same gate analysis on runs acquired on UPW targets, as shown in Fig. 4.

To obtain the net yield of the  $E_r = 64.5$  keV resonance we evaluated and subtracted the direct capture contribution to the observed count rate. An  $R$ -matrix fit [48] of all the available data [4,13–18] was performed to extrapolate the direct capture contribution to the astrophysical  $S$  factor [49] down to the resonance energy [50]. The branching ratios for the capture to different excited states were found to be constant over the energy range  $167 \leq E \leq 370$  keV [17]. Therefore, those same branchings were included in the simulation code to get the efficiency for the gate analysis,



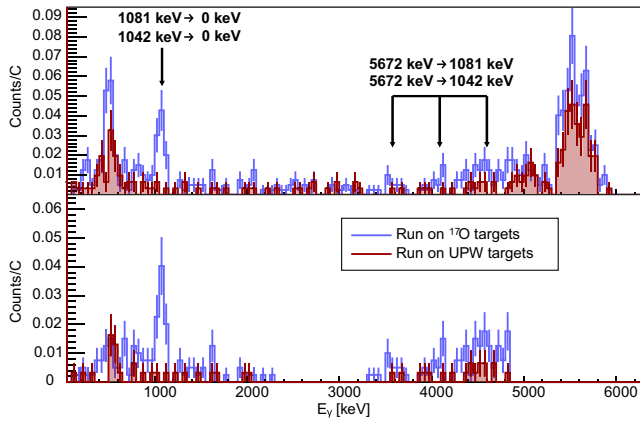


FIG. 4. Coincidence method applied to the  $^{17}\text{O}$  (blue) and UPW spectra (red). Top panel: events that add up to 5672 keV; the energies corresponding to the primary and secondary  $\gamma$  of the transition to 1081 keV are shown using arrows. Bottom panel: result of the secondary filter, only events belonging to the transition 5672 keV  $\rightarrow$  1081 keV are left in the chosen ROI; random coincidences survived the second filter and they were subtracted as estimated from the UPW measurement.

applied to the direct capture case. By combining the direct capture  $S$  factor from the  $R$  matrix fit and the efficiency from the simulation, we infer a 0.04 reactions/C direct capture yield a  $E_p = 80$  keV. This contribution is subtracted from the measured yield at that beam energy to obtain the yield due to the resonant reaction. The direct capture contributes to 8% of the measured experimental yield, see Eq. (2). This result was verified performing one measurement at  $E_p = 265$  keV, that falls within literature data [17,18], and one measurement at  $E_p = 142$  keV, to be compared with the  $R$ -matrix output. The measured  $S$  factors are  $S = (6.65 \pm 0.13)$  keVb and  $S = (6.40 \pm 0.40)$  keVb, respectively. These results are in agreement with previous experimental data and the new  $R$  matrix calculation.

The present result for the experimental yield is  $Y_{\text{exp}} = (0.50 \pm 0.10_{\text{stat}} \pm 0.04_{\text{syst}})$  reactions/C. In the statistical uncertainty we included the contribution from the beam induced background, the direct capture subtraction and the composition of  $^{17}\text{O}$  targets. The total systematic uncertainty accounts for uncertainty due to efficiency (3%), branchings (6%, see Fig. 1), stopping power uncertainty (4%) and charge integration (2%). We also included the uncertainty of the resonance strength at  $E_r = 183$  keV [17], used as the reference to determine the  $^{17}\text{O}$  isotopic abundance in targets.

Using the aforementioned yield we obtained a resonance strength of  $\omega\gamma_{(p,\gamma)} = (34 \pm 7_{\text{stat}} \pm 3_{\text{syst}})$  peV. A comparison with literature data is presented in Table I. The electron screening correction  $f = 1.15$  was derived considering the adiabatic approximation [26] resulting in a  $\omega\gamma_{(p,\gamma)}^{\text{bare}} = (30 \pm 6_{\text{stat}} \pm 2_{\text{syst}})$  peV. However, a recent work suggests that the screening correction in case of narrow resonances is negligible [51]. It must also be noted that a recent work reported

stopping powers for proton in Ta higher by 12% with respect to the SRIM database [52]. This would lead to an increase of the present effective stopping power, and consequently of the resonance strength, by 6%.

The present result for the resonance strength is the first obtained by a direct measurement and it is higher by a factor of  $\approx 2$  than values reported in literature. Using  $\Gamma_\gamma = 0.45(2)$  eV (the weighted mean of results in [22,27–29]),  $\Gamma_\alpha = 130(5)$  eV [24], see Table I, and the present resonance strength, a  $\Gamma_p = (39 \pm 8_{\text{stat}} \pm 3_{\text{syst}})$  neV [corresponding to  $\Gamma_p^{\text{bare}} = (34 \pm 7_{\text{stat}} \pm 3_{\text{syst}})$  neV] was calculated, in excellent agreement with the previous LUNA result reported in [25]. The weighted average of these two independent results yields  $\Gamma_p = 35(5)$  neV, which is inconsistent with the previous literature values, i.e., 19(3) [21] and 14(2) [20]. The present work confirms the evaluation of the strength of the 64.5 keV resonance in the  $\alpha$  channel reported in [25] and the astrophysical consequences discussed in [11,53].

In summary, we reported the first direct measurements of the 64.5 keV resonance strength and the direct capture contribution at 142 keV in  $^{17}\text{O}(p,\gamma)^{18}\text{F}$  reaction. To our knowledge this is the lowest strength value ever measured directly, corresponding to a cross section of 9.8 pb. The deep underground location of LUNA, the improvements to the setup, and the application of the gate analysis allowed us to achieve an outstanding sensitivity, opening the path to future challenging measurements. Our result for the resonance strength is roughly a factor of 2 higher than previous values reported in literature, suggesting also a higher  $\Gamma_p$ . The proton width calculated here is in excellent agreement with previous results by LUNA [25], improving our understanding of the  $^{16}\text{O}/^{17}\text{O}$  ratio measured in red-giant stars [7,8,54,55] and in O-reach presolar grains (for references see Fig. 3 of [56]). The full impact of the present new measurement on the uncertainty of the rates of the  $^{17}\text{O}(p,\alpha)^{14}\text{N}$  and  $^{17}\text{O}(p,\gamma)^{18}\text{F}$  reactions and their astrophysical implications will be discussed in a forthcoming work [50].

*Acknowledgments*—D. Ciccotti and the technical staff of the LNGS are gratefully acknowledged for their help during setup construction and data taking. Dr. Sara Carturan from LNL and the chemistry laboratory staff of LNGS are acknowledged for the help with target preparation. Financial support by INFN, the Italian Ministry of Education, University and Research (MIUR) (PRIN2022 CaBS, CUP:E53D230023 and SOCIAL, CUP: I53D23000840006) and through the “Dipartimenti di eccellenza” project “Science of the Universe,” the European Union (ERC Consolidator Grant project STARKEY, No. 615604, ERC-StG SHADES, No. 852016), [ELDAR UKRI ERC StG (EP/X019381/1)] and (ChETEC-INFRA, No. 101008324), Deutsche Forschungsgemeinschaft (DFG, BE 4100-4/1), the

Helmholtz Association (ERC-RA- 0016), the Hungarian National Research, Development and Innovation Office (NKFIH K134197), the European Collaboration for Science and Technology (COST Action ChETEC, CA16117) and the Hungarian Academy of Sciences via the Lendület Program LP2023-10. C. G. B., T. C., T. D., and M. A. acknowledge funding by STFC UK (Grant No. ST/L005824/1).

- [1] N. R. Hinkel *et al.*, *Astrophys. J. Suppl. Ser.* **226**, 4 (2016).
- [2] Energies are in the center-of-mass system unless specified differently.
- [3] M. Wang, W. J. Huang, F. G. Kondev, G. Audi, and S. Naimi, *Chin. Phys. C* **45**, 030003 (2021).
- [4] A. Chafa *et al.*, *Phys. Rev. C* **75**, 035810 (2007).
- [5] C. Iliadis, *Nuclear Physics of Stars* (Wiley-VCH, Weinheim, 2007).
- [6] M. J. Harris and D. L. Lambert, *Astrophys. J.* **285**, 674 (1984).
- [7] K. H. Hinkle, T. Lebzelter, and O. Straniero, *Astrophys. J.* **825**, 38 (2016).
- [8] T. Lebzelter, K. H. Hinkle, O. Straniero, D. L. Lambert, C. A. Pilachowski, and K. A. Nault, *Astrophys. J.* **886**, 117 (2019).
- [9] E. Zinner, in *Meteorites and Cosmochemical Processes*, edited by A. M. Davis (Elsevier, Amsterdam, 2014), Vol. 1, pp. 181–213.
- [10] S. Palmerini, S. Cristallo, L. Piersanti, D. Vescovi, and M. Busso, *Universe* **7**, 175 (2021).
- [11] M. Lugaro *et al.*, *Nat. Astron.* **1**, 0027 (2017).
- [12] D. R. Tilley, H. R. Weller, C. M. Cheves, and R. M. Chasteler, *Nucl. Phys.* **A595**, 1 (1995).
- [13] C. Fox, C. Iliadis, A. E. Champagne, R. P. Fitzgerald, R. Longland, J. Newton, J. Pollanen, and R. Runkle, *Phys. Rev. C* **71**, 055801 (2005).
- [14] A. Chafa *et al.*, *Phys. Rev. Lett.* **95**, 031101 (2005).
- [15] U. Hager *et al.*, *Phys. Rev. C* **85**, 035803 (2012).
- [16] A. Kontos *et al.*, *Phys. Rev. C* **86**, 055801 (2012).
- [17] A. Di Leva *et al.* (LUNA Collaboration), *Phys. Rev. C* **89**, 015803 (2014).
- [18] M. Q. Buckner, C. Iliadis, K. J. Kelly, L. N. Downen, A. E. Champagne, J. M. Cesaratto, C. Howard, and R. Longland, *Phys. Rev. C* **91**, 015812 (2015).
- [19] J. C. Blackmon, A. E. Champagne, M. A. Hofstee, M. S. Smith, R. G. Downing, and G. P. Lamaze, *Phys. Rev. Lett.* **74**, 2642 (1995).
- [20] M. L. Sergi *et al.*, *Phys. Rev. C* **91**, 065803 (2015).
- [21] C. Iliadis, R. Longland, A. Champagne, and A. Coc, *Nucl. Phys.* **A841**, 251 (2010).
- [22] I. Berka, K. P. Jackson, C. Rolfs, A. M. Charlesworth, and R. E. Azuma, *Nucl. Phys.* **A288**, 317 (1977).
- [23] G. Bogaert, V. Landré, P. Aguer, S. Barhoumi, M. Kious, A. Lefebvre, J. P. Thibaud, and D. Bertault, *Phys. Rev. C* **39**, 265 (1989).
- [24] H. B. Mak, G. T. Ewan, H. C. Evans, J. D. MacArthur, W. McLatchie, and R. E. Azuma, *Nucl. Phys.* **A343**, 79 (1980).
- [25] C. G. Bruno *et al.*, *Phys. Rev. Lett.* **117**, 142502 (2016).
- [26] H. J. Assenbaum, K. Langanke, and C. Rolfs, *Z. Phys. A Hadrons Nucl.* **327**, 461 (1987).
- [27] P. D. Parker, *Phys. Rev.* **173**, 1021 (1968).
- [28] C. Rolfs, A. M. Charlesworth, and R. E. Azuma, *Nucl. Phys.* **A199**, 257 (1973).
- [29] H. W. Becker, W. E. Kieser, C. Rolfs, H. P. Trautvetter, and M. Wiescher, *Z. Phys. A Hadrons Nucl.* **305**, 319 (1982).
- [30] M. D. Hannam and W. J. Thompson, *Nucl. Instrum. Methods Phys. Res., Sect. A* **431**, 239 (1999).
- [31] A. Caciolli *et al.*, *Eur. Phys. J. A* **39**, 179 (2009).
- [32] A. Boeltzig *et al.*, *J. Phys. G* **45**, 025203 (2018).
- [33] J. Skowronski *et al.*, *J. Phys. G Nucl. Phys.* **50**, 045201 (2023).
- [34] A. Formicola *et al.*, *Nucl. Instrum. Methods Phys. Res., Sect. A* **507**, 609 (2003).
- [35] J. Skowronski *et al.*, *Phys. Rev. Lett.* **131**, 162701 (2023).
- [36] A. Caciolli *et al.*, *Eur. Phys. J. A* **48**, 144 (2012).
- [37] A. Best *et al.*, *Phys. Lett. B* **797**, 134900 (2019).
- [38] F. R. Pantaleo *et al.*, *Phys. Rev. C* **104**, 025802 (2021).
- [39] J. F. Ziegler, *Nucl. Instrum. Methods Phys. Res., Sect. B* **219**, 1027 (2004).
- [40] A. Boeltzig *et al.*, *Phys. Lett. B* **795**, 122 (2019).
- [41] F. Ferraro *et al.*, *Phys. Rev. Lett.* **121**, 172701 (2018).
- [42] S. Agostinelli *et al.*, *Nucl. Instrum. Methods Phys. Res., Sect. A* **506**, 250 (2003).
- [43] E. G. Adelberger *et al.*, *Rev. Mod. Phys.* **83**, 195 (2011).
- [44] T. Asakawa, D. Nagano, H. Miyazawa, and I. Clark, *J. Vac. Sci. Technol. B* **38**, 034008 (2020).
- [45] F. Ferraro *et al.*, *Eur. Phys. J. A* **54**, 44 (2018).
- [46] D. Piatti *et al.*, *Eur. Phys. J. A* **58**, 194 (2022).
- [47] L. Zhang *et al.*, *Nature (London)* **610**, 656 (2022).
- [48] R. E. Azuma *et al.*, *Phys. Rev. C* **81**, 045805 (2010).
- [49]  $S(E) = E\sigma(E) \exp[2\pi\eta(E)]$ , where  $E$  is the energy in the center of mass frame,  $\sigma(E)$  is the cross section, and  $\eta(E)$  is the Sommerfeld parameter [5].
- [50] D. Rapagnani *et al.* (to be published).
- [51] C. Iliadis, *Phys. Rev. C* **107**, 044610 (2023).
- [52] M. V. Moro, P. Bauer, and D. Primetzhofer, *Phys. Rev. A* **102**, 022808 (2020).
- [53] O. Straniero *et al.*, *Astron. Astrophys.* **598**, A128 (2017).
- [54] T. Lebzelter, O. Straniero, K. H. Hinkle, W. Nowotny, and B. Aringer, *Astron. Astrophys.* **578**, A33 (2015).
- [55] R. De Nutte *et al.*, *Astron. Astrophys.* **600**, A71 (2017).
- [56] C. Floss and P. Haenecour, *Geochem. J.* **50**, 3 (2016).